Chinese Chemical Letters 34 (2023) 108784

Contents lists available at ScienceDirect

Chinese Chemical Letters

journal homepage: www.elsevier.com/locate/cclet

Highlight

Molecular engineering of carbon nitrides for overall photosynthesis of H_2O_2

Jin Ma, Xiaoxiao Peng, Zhixin Zhou*, Yanfei Shen*, Yuanjian Zhang*

Jiangsu Engineering Laboratory of Smart Carbon-Rich Materials and Device, Jiangsu Province Hi-Tech Key Laboratory for Bio-Medical Research, School of Chemistry and Chemical Engineering, Medical School, Southeast University, Nanjing 211189, China

ARTICLE INFO

Article history:
Received 18 April 2023
Revised 7 June 2023
Accepted 5 July 2023
Available online 6 July 2023

Keywords:
Carbon nitrides
Photocatalysts
H_2O_2 production
Oxygen reduction reaction
Water oxidation reaction

ABSTRACT

Artificial photocatalysis offers a promising strategy to sustainably produce hydrogen peroxide (H_2O_2) that is one of the most valuable multifunctional chemicals. Among various photocatalysts, polymeric carbon nitride (pCN) has drawn continuous attention in non-sacrificial H_2O_2 production. However, the poor activity of half reactions, *i.e.*, the oxygen reduction reaction (ORR) and water oxidation reaction (WOR), greatly restricts the efficiency of photocatalytic H_2O_2 production. In this highlight, we discuss the significant advances in molecular engineering of carbon nitrides for H_2O_2 photosynthesis and the importance of the deep understanding of the photocatalysis process for rational design and reaction pathways of organic conjugated polymers to address the growing H_2O_2 demand. Furthermore, we summarize the emerging applications of photocatalytic H_2O_2 productions beyond energy and environment.

Hydrogen peroxide (H_2O_2) is one of the most valuable multifunctional chemicals with widespread applications. Currently, the well-established industrial anthraquinone-based method for H_2O_2 production is energy-intensive and environmentally unfriendly [1]. In addition to eco-friendly and economical electrochemical methods [2], artificial photosynthetic H_2O_2 generation is also considered as a clean and energy-saving approach that has attracted significant interest. Substantial efforts have been devoted to developing new photocatalysts with high efficiency, good selectivity, and stability [3]. Visible-light-responsive organic polymers [4], such as polymeric carbon nitrides, have been widely investigated as potential catalysts for H_2O_2 photosynthesis because of their high physical and chemical stability, low cost, and adjustable electronic bandgaps.

In 2014, Shiraishi *et al.* first reported that graphitic carbon nitride (g-C_3N_4) could produce H_2O_2 under photoirradiation using alcohol as an electronic donor [5]. Inspired by this seminal work, numerous polymeric carbon nitride-based photocatalysts have emerged in recent years for the photocatalytic production of H_2O_2, especially for solar-driven H_2O_2 production without any sacrificial agents [6]. However, most carbon nitride materials cannot produce effective holes or form active surface sites to directly oxidize H_2O into H_2O_2, and tend to undergo the thermodynamically favorable $4e^-$ WOR process [7]. Molecular engineering of carbon nitrides, including heteroatom doping (*e.g.*, P or Sb) [8], modifying heteromolecules (*e.g.*, pyromellitic diimide or biphenyl diimide) [9], surface defect engineering (*e.g.*, C≡N groups and N vacancies) [10], and modulating triazine/heptazine based frameworks (*e.g.*, by spatially separated redox centers) [11,12], plays a key role in the formation of architectures with great topologies [13]. Indeed, some substantial significant advances have been made to improve the non-sacrificial ORR and WOR efficiency for H_2O_2 photosynthesis; however, the efficiency and stability of current state-of-the-art photocatalysts are still low.

Each half-reaction includes different reaction pathways determined by the electron transfer number (Fig. 1a) [14–16]. For ORR half-reaction, the direct two-electron process exhibits a thermodynamically more favorable energy level (+0.695 V *vs.* NHE) and the indirect stepwise single-electron reduction firstly reduce O_2 to form hydroperoxyl radicals (·OOH, −0.05 V *vs.* NHE) which then couple with protons to generate H_2O_2 (+1.44 V *vs.* NHE). For the WOR half-reaction, H_2O can be directly oxidized by two holes to form H_2O_2 (+1.76 V *vs.* NHE), and the stepwise single-electron WOR process requires high concentrations of hydroxyl radicals (·OH, +2.73 V *vs.* NHE) to form the desired H_2O_2. Theoretically, based on the combination of different ORR and WOR pathways, there are four different pathways for the overall photosynthesis of H_2O_2: $2e^-$ ORR and $4e^-$ WOR pathways [8], stepwise $1e^-$ ORR and $4e^-$ WOR pathways [10], stepwise $1e^-$ ORR and $1e^-$ WOR pathways [17], and $2e^-$ ORR and $2e^-$ WOR pathways [11,12,18,19],

* Corresponding authors.
E-mail addresses: Zhixin.Zhou@seu.edu.cn (Z. Zhou), Yanfei.Shen@seu.edu.cn (Y. Shen), Yuanjian.Zhang@seu.edu.cn (Y. Zhang).

https://doi.org/10.1016/j.cclet.2023.108784
1001-8417/

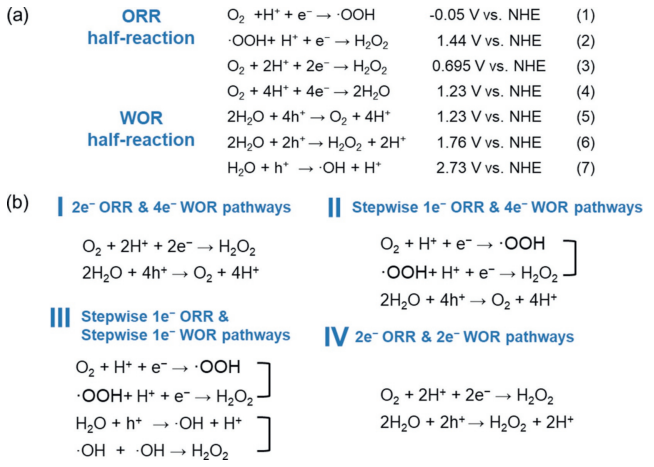

Fig. 1. (a) Reaction scheme for photocatalytic H_2O_2 production and the corresponding energy diagrams for the ORR and WOR pathways. (b) Four classical combinations of ORR and WOR pathways for the overall photosynthesis of H_2O_2. Reprint with permission [14,15]. Copyright 2022, ACS.

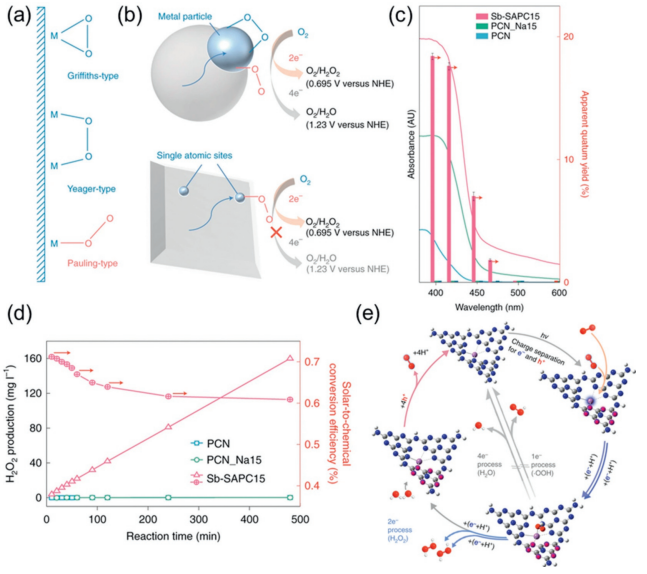

Fig. 2. (a) Schematic structures of O_2 adsorption on metal surface. (b) ORR mechanism on a metal particle (top) and isolated atomic site (bottom). (c) Action spectra of PCN, PCN_Na15, and Sb-SAPC15 towards H_2O_2 production in phosphate buffer solution. (d) Solar-to-chemical conversion efficiencies of PCN, PCN_Na15, and Sb-SAPC15 under AM 1.5, illumination in a phosphate buffer solution. (e) Reaction mechanism of CN with Sb sites for photocatalytic H_2O_2 production. The white, gray, blue, red and magenta spheres refer to hydrogen, carbon, nitrogen, oxygen and Sb atoms, respectively. Reprint with permission [8]. Copyright 2021, Nature.

which provide potent guidance for the design of photocatalytic processes (Fig. 1b) [14].

The creation of heteroatom-doped photocatalysts is an essential strategy in the pursuit of advanced photocatalytic processes. In an elegant study, Ohno *et al.* reported a Sb single-atom carbon nitride photocatalyst (Sb-SAPC) for non-sacrificial photocatalytic H_2O_2 synthesis under ambient conditions [8]. The introduction of highly active and selective Sb sites for the $2e^-$ ORR to consume the O_2 generated from $4e^-$ WOR in the photocatalytic system offers a high yield and selectivity for H_2O_2 photosynthesis (Figs. 2a and b), with an apparent quantum yield of 17.6% at 420 nm (Fig. 2c), together with a solar-to-chemical conversion (SCC) efficiency of 0.61% (Fig. 2d) for H_2O_2 synthesis. The d^{10} electronic configuration of Sb single-atom sites produces a new O–O stretching mode in the Sb–OOH species with an end-on adsorption configuration ap-

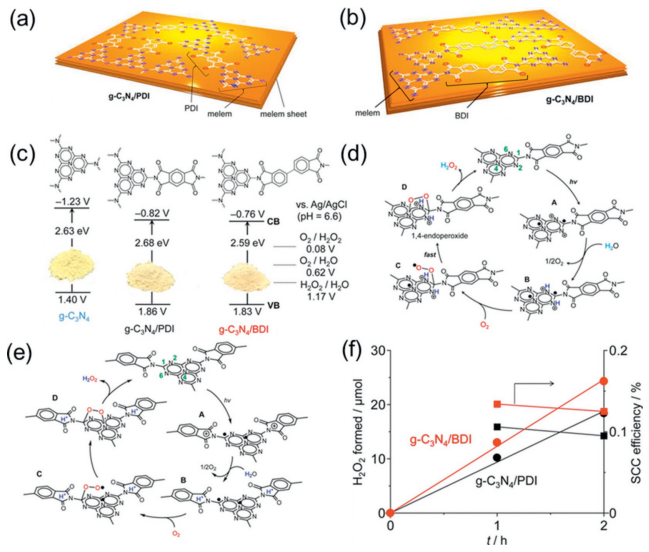

Fig. 3. (a) Molecular structure of g-C_3N_4/PDI. (b) Molecular structure of g-C_3N_4/BDI. (c) Electronic band structures of g-C_3N_4, g-C_3N_4/PDI, and g-C_3N_4/BDI. (d) Mechanism of g-C_3N_4/PDI for photocatalytic H_2O_2 production in pure water. (e) Mechanism of g-C_3N_4/BDI for photocatalytic H_2O_2 production in pure water system. (f) Change in the amount of H_2O_2 formed and SCC efficiency under simulated AM1.5 G sunlight (1 sun) with time. Reprint with permission [9]. Copyright 2016, ACS.

pearing under photo-irradiation, which reduces the possibility of O–O bond breaking and enhances the trapping of photogenerated electrons for the $2e^-$ ORR. Moreover, these sites are energetically unfavorable for the side hydrogen evolution reactions. In contrast, the photogenerated holes were concentrated at the N atoms in the *s*-heptazine moiety next to the Sb site to catalyze the $4e^-$ WOR. Both the $2e^-$ ORR and $4e^-$ WOR pathways formed a prime overall photosynthesis of H_2O_2 (Fig. 2e). Further examples of Ga- and Co-doped carbon nitrides also proved that the single atoms in carbon nitride certainly tailor the electronic structure and induce charge redistribution. It was supposed to not only promote the separation/transfer of charge carriers and the absorption/activation of O_2 in the $2e^-$ ORR reaction but also effectively enhance the $2e^-/4e^-$ WOR reaction [19,20].

In addition to heteroatom doping, incorporating heteromolecules, such as aromatic diimides, an important class of n-type organic semiconductors with high electron mobility and stability, also positively adjusts the electronic structure and shifts the oxidation and reduction potentials, owing to their high electron affinity [9]. It has been demonstrated that the VB position of g-C_3N_4 is not thermodynamically feasible for the concurrent WOR. The introduction of pyromellitic diimide (PDI, Fig. 3a) and biphenyl diimide (BDI, Fig. 3b) into the g-C_3N_4 structure can generally positively shift the CB and VB positions and improve the thermodynamic driving force for catalyzing the O_2 evolution reaction (Fig. 3c). Figs. 3d and e show the reaction pathways for the overall photosynthesis of H_2O_2 *via* the coupling of the $2e^-$ ORR pathway with the $4e^-$ WOR pathway on g-C_3N_4/PDI and g-C_3N_4/BDI. Accordingly, g-C_3N_4/PDI and g-C_3N_4/BDI exhibited considerable H_2O_2 production rates without sacrificial agents in a pure water system, and the average SCC efficiencies of the optimized g-C_3N_4/PDI and g-C_3N_4/BDI reached 0.10% and 0.13%, respectively (Fig. 3f).

Furthermore, engineering defects on a photocatalyst surface is a universal and powerful method for improving the photocatalytic conversion efficiency. Recently, Zheng *et al.* sequentially introduced the –C≡N groups and N vacancies into g-C_3N_4 (N_v–C≡N–CN, Fig. 4a) [10]. The synergistic effect of the dual defect sites enhanced the visible-light absorption (Fig. 4b) and carrier separation capabilities (Fig. 4c). Besides, it has been verified that N vacan-

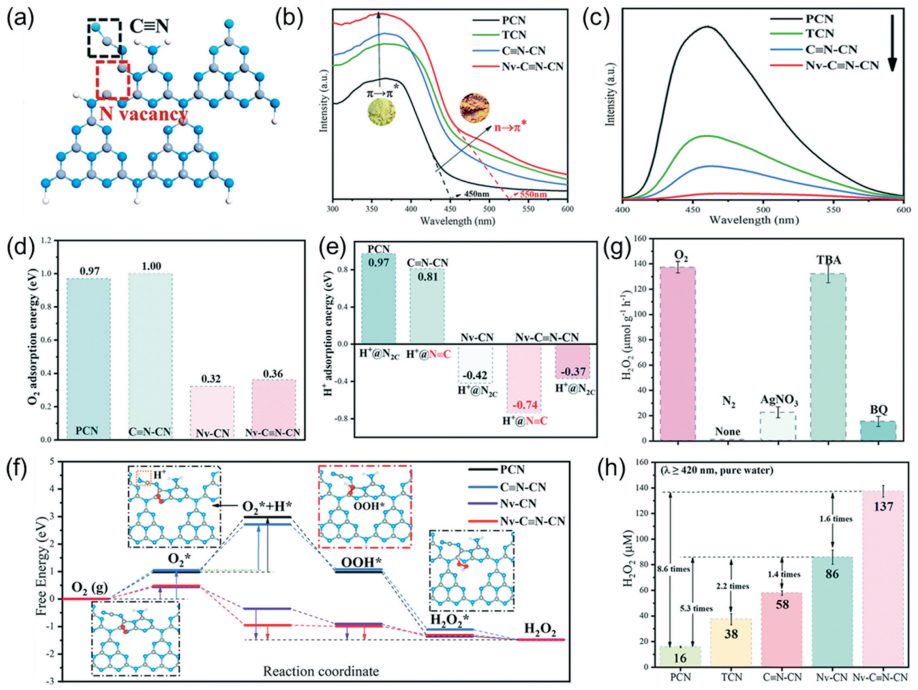

Fig. 4. (a) Defect structure in g-C_3N_4 heptazine units. Inset: C≡N groups and N vacancies. (b) UV–Vis DRS of all samples. Inset: Photographs of PCN and N_v–C≡N–CN. (c) Photoluminescence (PL) spectra of all samples. (d) O_2 adsorption energy and (e) H^+ adsorption energy on g-C_3N_4 with different defect models. (f) Free energy profiles for photocatalytic H_2O_2 evolution reactions over PCN, C≡N–CN, N_v–CN, and N_v–C≡N–CN. (g) Photocatalytic H_2O_2 generation rates of N_v–C≡N–CN under different reaction gasses or sacrificial agents. (h) Comparison of photocatalytic H_2O_2 generation activity of different samples under the same conditions in a pure water system. Reprint with permission [10]. Copyright 2022, RSC.

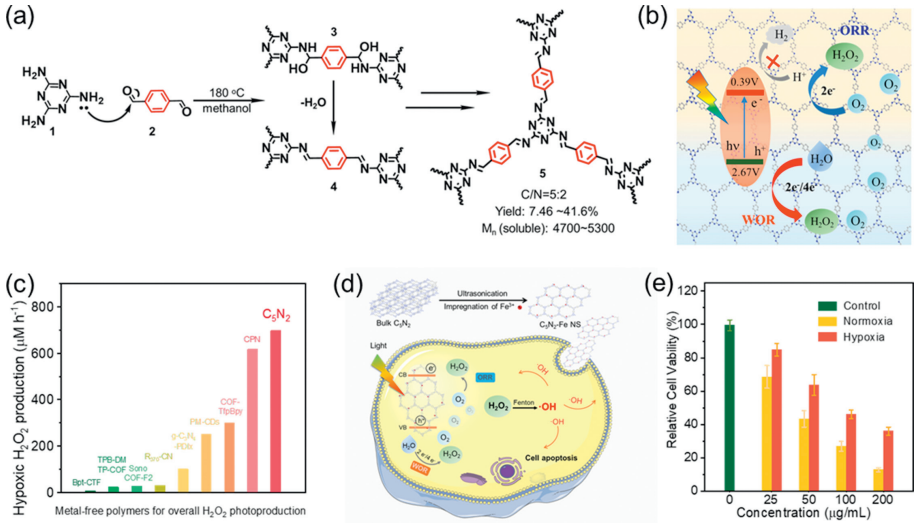

Fig. 5. (a) Conjugated linker formation in the synthesis of C_5N_2 (**5**) from melamine (**1**) and *p*-phthalaldehyde (**2**) *via* Schiff base reactions. (b) Bandgap position of C_5N_2 and mechanism of photocatalytic H_2O_2 production by C_5N_2. Inset: C=N linkage in C_5N_2. (c) Summary of the photocatalytic activity for H_2O_2 production in a hypoxic microenvironment using different metal-free polymers in the literature. (d) Therapeutic processes using C_5N_2 to generate ·OH *via* the Fenton reaction under light irradiation in hypoxic environments. (e) Cell viability assay of C_5N_2–Fe–NS-treated 4T1 cells under light irradiation in hypoxic and normoxic environments. Reprint with permission [12]. Copyright 2022, Wiley.

cies can effectively adsorb and activate O_2 (Fig. 4d), while the C≡N groups enhance the adsorption of H^+ (Fig. 4e), which synergistically promotes the formation and hydrogenation of OOH* to H_2O_2 (Fig. 4f). Accordingly, the N_v–C≡N–CN group achieved overall photosynthesis of H_2O_2 in pure water *via* concurrent stepwise single-electron ORR and four-electron WOR pathways (Fig. 4g). Meanwhile, the N_v–C≡N–CN photocatalyst exhibited 8.5 times H_2O_2 production rates higher than pristine bulk carbon nitrides without sacrificial agents, leading to a significant SCC efficiency of 0.23% (Fig. 4h).

Expect for the above-mentioned engineering of g-C_3N_4, the modulation of triazine/heptazine-based frameworks has great potential for the photocatalytic synthesis of H_2O_2. Rationally designed monomers for pre-assembly and precise regioselective coupling polymerization play key roles in the formation of architectures with separated redox centers. Very recently, Zhang *et al.* modulated a triazine-based framework with spatially separated redox centers and reported well-defined C_5N_2 with a conjugated C=N linkage to photosynthesize H_2O_2 from H_2O without sacrificial agents under hypoxic conditions (Fig. 5a) [12]. Compared with

the tertiary N linkage in g-C_3N_4 breaking the conjugation over the heptazine rings, the conjugated linkers were redistributed in the C_5N_2 units, resulting in the strengthened delocalization of π-electrons, which downshifted the CB and VB positions. C_5N_2 with unusually low conduction (>0 V *vs*. NHE) and valence band positions promoted realistic selectivity in thermodynamics and high activity in kinetics for overall H_2O_2 photosynthesis through synergistic $2e^-$ ORR and $2/4e^-$ WOR (Fig. 5b), and C_5N_2 demonstrated the highest H_2O_2 photocatalytic activity (698 $\mu mol\,L^{-1}\,h^{-1}$) under hypoxic conditions among the polymeric photocatalysts (Fig. 5c). For the first time, C_5N_2 was successfully applied to hypoxic/normoxic tumor photodynamic therapy/chemodynamic therapy (PDT/CDT) (Fig. 5d) and exhibited competitive performance under hypoxic and normoxic conditions (Fig. 5e). These results indicate that C_5N_2 offers an opportunity to potentially cut the cost of H_2O_2 production in a large scale and opens new avenues for highly efficient and selective H_2O_2 photosynthesis, particularly under hypoxic conditions in biomedical therapy systems.

Although previous studies have been devoted to enhancing the SCC efficiency toward solar-driven H_2O_2 production *via* the design of polymer photocatalysts, the efficiency of non-sacrificial H_2O_2 generation has not yet fulfilled the industrial requirements. Thus, the technical and economic feasibility of H_2O_2 photosynthesis should be rigorously analyzed. Apart from the wide use of H_2O_2 in the energy field owing to its high energy density, its strong oxidation power, and endogenous nature may achieve a potential application in environmental and biomedical fields, such as coupling solar-driven H_2O_2 production with dye degradation [18], conversion of organic molecules [21], bacterial disinfection [22], and cancer therapy [12], which could potentially lower the cost of large-scale production of H_2O_2.

In summary, we highlight the significant advances in H_2O_2 photosynthesis in the molecular engineering of carbon nitrides, a deep understanding of the photocatalysis process for the rational design and reaction pathways of carbon nitrides, and the technical and economical emerging applications of classical examples to address the growing H_2O_2 demand. The high energy density, strong oxidation power, and endogenous nature of H_2O_2 make it potentially applicable in energy, environmental, and biomedical fields by coupling solar-powered technologies for H_2O_2 production with carbon nitride. Furthermore, other potential catalysts, such as organic conjugated polymer resorcinol formaldehyde resins with a low bandgap, also exhibit outstanding efficiency without sacrificial reagents for the overall photosynthesis of H_2O_2 [3,23].

Declaration of competing interest

The authors declare that they have no known competing financial interests or personal relationships that could have appeared to influence the work reported in this paper.

Acknowledgment

This research was supported by the National Natural Science Foundation of China (Nos. 22174014 and 22074015).

References

[1] C. Xia, Y. Xia, P. Zhu, L. Fan, H. Wang, Science 366 (2019) 226–231.
[2] X. Hu, Z. Sun, G. Mei, et al., Adv. Energy Mater. 12 (2022) 2201466.
[3] Y. Shiraishi, T. Takii, T. Hagi, et al., Nat. Mater. 18 (2019) 985–993.
[4] H. Yang, Z. Wang, S. Liu, Y. Shen, Y. Zhang, Chin. Chem. Lett. 31 (2020) 3047–3054.
[5] Y. Shiraishi, S. Kanazawa, Y. Kofuji, et al., Angew. Chem. Int. Ed. 53 (2014) 13454–13459.
[6] Y. Kofuji, Y. Isobe, Y. Shiraishi, et al., J. Am. Chem. Soc. 138 (2016) 10019–10025.
[7] H. Zhao, Q. Jin, M.A. Khan, et al., Chem. Catal. 2 (2022) 1720–1733.
[8] Z. Teng, Q. Zhang, H. Yang, et al., Nat. Catal. 4 (2021) 374–384.
[9] Y. Kofuji, S. Ohkita, Y. Shiraishi, et al., ACS Catal. 6 (2016) 7021–7029.
[10] X. Zhang, P. Ma, C. Wang, et al., Energy Environ. Sci. 15 (2022) 830–842.
[11] H. Cheng, H. Lv, J. Cheng, et al., Adv. Mater. 34 (2022) e2107480.
[12] J. Ma, X. Peng, Z. Zhou, et al., Angew. Chem. Int. Ed. 61 (2022) e202210856.
[13] H. Hou, X. Zeng, X. Zhang, Angew. Chem. Int. Ed. 59 (2020) 17356–17376.
[14] H. Cheng, J. Cheng, L. Wang, H. Xu, Chem. Mater. 34 (2022) 4259–4273.
[15] J.J. Gao, B. Liu, ACS Mater. Lett. 2 (2020) 1008–1024.
[16] Y. Sun, L. Han, P. Strasser, Chem. Soc. Rev. 49 (2020) 6605–6631.
[17] Y. Liu, X. Zeng, X. Hu, et al., Catal. Today 335 (2019) 243–251.
[18] M. Kou, Y. Wang, Y. Xu, et al., Angew. Chem. Int. Ed. 61 (2022) 1521–3773.
[19] H. Tan, P. Zhou, M. Liu, et al., Nat. Synth. 2 (2023) 557–563.
[20] W. Wang, Q. Song, Q. Luo, et al., Nat. Commun. 14 (2023) 2493.
[21] Y. Zhang, C. Pan, G. Bian, et al., Nat. Energy 8 (2023) 361–371.
[22] W. Wang, H. Xie, G. Li, et al., ACS ES&T Water 1 (2021) 1483–1494.
[23] C. Zhao, X. Wang, Y. Yin, et al., Angew. Chem. Int. Ed. 62 (2023) e202218318.